Title

Indoor-Generated PM2.5 During COVID-19 Shutdowns Across California: Application of the PurpleAir Indoor–Outdoor Low-Cost Sensor Network

Journal

Environmental Science and Technology, 55(9)

ISSN

0013-936X

Authors

Mousavi, Amirhosein
Wu, Jun

Publication Date

2021-05-04

DOI

10.1021/acs.est.0c06937

Peer reviewed

HHS Public Access

Author manuscript

Environ Sci Technol. Author manuscript; available in PMC 2022 May 04.

Published in final edited form as:

Environ Sci Technol. 2021 May 04; 55(9): 5648–5656. doi:10.1021/acs.est.0c06937.

Indoor-Generated $PM_{2.5}$ During COVID-19 Shutdowns Across California: Application of the PurpleAir Indoor–Outdoor Low-Cost Sensor Network

Amirhosein Mousavi,

Department of Environmental and Occupational Health, Program in Public Health, Susan and Henry Samueli College of Health Sciences, University of California, Irvine, Irvine, California 92697, United States;

Jun Wu

Department of Environmental and Occupational Health, Program in Public Health, Susan and Henry Samueli College of Health Sciences, University of California, Irvine, Irvine, California 92697, United States;

Abstract

Although evidences showed an overall reduction in outdoor air pollution levels across the globe due to COVID-19-related lockdown, no comprehensive assessment was available for indoor air quality during the period of stay-at-home orders, despite that the residential indoor environment contributes most to personal exposures. We examined temporal and diurnal variations of indoor $PM_{2.5}$ based on real-time measurements from 139 indoor–outdoor co-located low-cost PurpleAir sensor sets across California for pre-, during, and post-lockdown periods in 2020 and "business-as-usual" periods in 2019. A two-step method was implemented to systematically control the quality of raw sensor data and calibrate the sensor data against co-located reference instruments. During the lockdown period, 17–24% higher indoor $PM_{2.5}$ concentrations were observed in comparison to those in the 2019 business-as-usual period. In residential sites, a clear peak in $PM_{2.5}$ concentrations in the afternoon and elevated evening levels toping at roughly 10 $\mu g \cdot m^{-3}$ was observed, which reflects enhanced human activity during lunch and dinner time (i.e., cooking) and possibly more cleaning and indoor movement that increase particle generation and resuspension in homes. The contribution of indoor-generated $PM_{2.5}$ to total indoor concentrations increased as high as 80% during and post-lockdown periods compared to before lockdown.

Corresponding Author: **Jun Wu –** Department of Environmental and Occupational Health, Program in Public Health, Susan and Henry Samueli College of Health Sciences, University of California, Irvine, Irvine, California 92697, United States; junwu@hs.uci.edu.

Supporting Information

The Supporting Information is available free of charge at https://pubs.acs.org/doi/10.1021/acs.est.0c06937.

Fractions of discarded data after quality control (Table S1); multisensor house location (Figure S1); human daily mobility in California during the outbreak of COVID-19 (Figure S2); county-level human daily mobility by categorized place at the county level in California during the outbreak of COVID-19 (Figure S3); comparison of indoor and outdoor $PM_{2.5}$ levels in the pre-lockdown period in 2020 and in the same time period in 2019 (Figure S4); and example of multiple indoor sensor monitoring in different parts of a house (Figure S5) (PDF)

Complete contact information is available at: https://pubs.acs.org/10.1021/acs.est.0c06937

The authors declare no competing financial interest.

Graphical Abstract

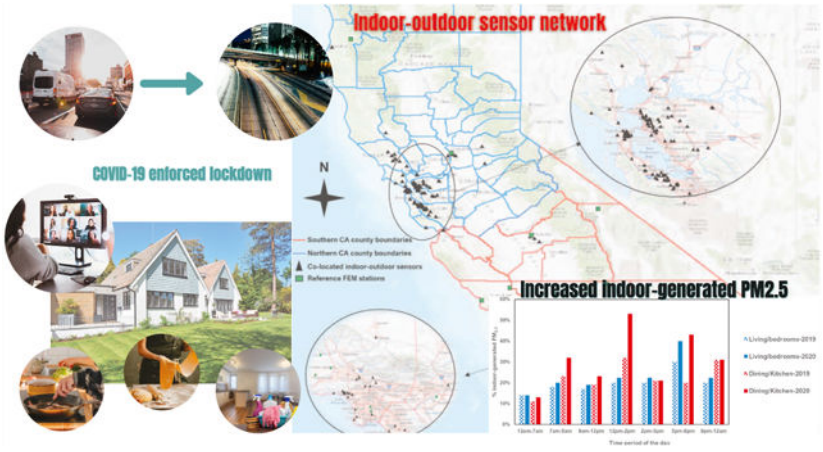

1. INTRODUCTION

Temporary air pollution reduction during the COVID-19 lockdown was a unique natural experiment to learn and examine sudden changes in emission-related activity patterns and their impact on air quality and long-term climate change improvements.[1–3] Although there is evidence that COVID-19 related closures have reduced ambient air pollution levels and may decrease associated long-term and short-term health impacts across the globe,[4–6] there is a lack of comprehensive assessment of indoor air quality changes during the period of stay-at-home orders, despite that residential indoor environment contributes most to personal exposures because people spend the most time at home indoors. While a natural reduction in the emissions of particulate matter (PM) and co-pollutants including carbon monoxide, carbon dioxide, and nitrogen oxides from outdoor urban activities is important from a climatological and environmental health perspective, indoor emission sources attributable to household activities are more pronounced in terms of personal exposure to air pollution and associated detrimental health effects.[7–11]

World Health Organization (WHO) reports that each year, close to 4 million people die prematurely from illness attributable to household air pollution.[7] Further, close to half of deaths due to pneumonia among children under 5 years of age are caused by PM compounds (e.g., soot) inhaled from household air pollution. During the lockdown period, people spend more time in the residential indoor environment, which makes indoor air quality more important than ever. Emissions of indoor pollutants may likely increase due to more cooking, cleaning, smoking, and other activities indoors from remote working/learning. Susceptible subpopulations, including children, the elderly, and individuals with preexisting conditions, may suffer even more from indoor pollution than the general population as they tend to stay at home more to avoid outdoor contact and minimize the risk of virus infection. Further, households of low socioeconomic status (SES) may share a disparate burden of indoor pollution exposure as they may live in small and crowded apartments with more indoor sources. The COVID-19 lockdown interventions are an opportunity to investigate indoor air quality and potential indoor sources, especially in low SES communities.

The recent rise in deployment of low-cost sensors in urban and rural communities has enabled new approaches to monitor and investigate air quality in higher spatiotemporal resolutions that cannot be afforded by regulatory agency monitors.[8] Usage of the PurpleAir low-cost sensor network in indoor and outdoor settings[8] has also created a unique opportunity to fill the gap in comprehensive understanding of the impact of COVID lockdown on indoor air quality at a large scale. However, concerns exist regarding the uncertainty and malfunctions (i.e., wireless communications loss, power outages, or other measurement interferences) of the low-cost PurpleAir sensor data as well as potential biases due to environmental conditions, which requires a systematic post-process approach to ensure sensor data quality, especially in long-term studies.[9–12] While most of the previous studies suggest calibration of the PurpleAir sensor data to the nearest reference monitor with a correction factor as a result of multivariate regression accounting for environmental (e.g., relative humidity and temperature) and operational factors (i.e., indoor vs outdoor and sensor uptime after deployment),[12–15] a recent study in Los Angeles County[16] has developed a systematic multistep quality control scheme using the readings from both of the sensor channels to minimize outliers and eliminate readings from malfunctioning sensors.

To understand the influence of stay-at-home orders on both indoor and outdoor air quality, we analyzed indoor and outdoor PM < 2.5 μm ($PM_{2.5}$) concentrations from the co-located indoor and outdoor low-cost real-time PurpleAir sensor network across California. We compared $PM_{2.5}$ concentrations pre-, during, and post-COVID-19 closures in 2020 and 2019 (business as usual). Temporal and diurnal variation of indoor-generated $PM_{2.5}$ were also examined based on location (northern vs southern California), type of buildings (residential vs office/school), and proximity to road emissions (remote background vs high traffic).

2. DATA COLLECTION AND ANALYSIS

2.1. Study Domain and Time Periods.

We have restricted our study domain to California, a state that has around 40 million population and covers roughly 164 000 $mile^2$ area. We separated the study area into northern and southern California subregions with slightly different traffic density and ambient $PM_{2.5}$ levels[13,14] (Figure 1). In each region, co-located indoor and outdoor sensors (i.e., deployed in the same residential/office/school unit) were identified. Although most of indoor–outdoor pairs only had one indoor sensor, one house located at Aromas, Monterey County, had multiple indoor sensors that allowed a closer investigation of $PM_{2.5}$ distribution in different indoor locations (Section 3.5). The co-located sites were overlaid with Google maps, which provided land-use and type of building (e.g., residence, commercial building, office, and school) information that was furthered assigned to each individual site (Figure 1).

Remote-background and near-road sites were identified based on their proximity to major roads (freeway, highway, or main street) with annual average daily traffic (AADT) > 90 000 vehicles per day[15] or airport. “Near-road” sites were classified as those within 50 m of the edge of a major road. No co-located site was within 15 km downwind of an airport. Table 1 shows the number of co-located sites by the subregion, type of building, and proximity to the road.

We restricted our analysis to data from the first of January to the end of July in both 2020 and 2019 ("business-as-usual" period as a reference). We compared daily $PM_{2.5}$ concentrations during the same period in 2020 vs 2019 and the concentrations before the stay-at-home order (January 1–March 16, 2020),[17] during the lockdown period (March 17–May 5, 2020),[17] and during the first stage of state reopening (May 6–July 30, 2020).[17] The majority of the population worked and/or schooled from home since the statewide lockdown and stay-at-home order on March 15, 2000 till the first-stage state reopening order on May 5, 2020.[17] Even after the reopening when the essential business went back to normal, guidelines were still in place that restricted gathering and a large percentage of the population continued working/schooling from home across the state.

2.2. PurpleAir Sensor Network.

PurpleAir is a low-cost sensor monitor and has started to be deployed in the U.S. and worldwide since 2017. The latest model (PA-II-SD) contains two PMS5003 sensors (Plantower, Beijing, China), which estimate particle mass concentrations by measuring the amount of light scattered at ~680 nm.[10,16] Initial assessment of the PMS5003 sensors by South Coast Air Quality Management District (AQ-SPEC team)[18] showed low intra-model variability; $PM_{2.5}$ sensor data correlated very well with the corresponding reference monitor measurements (R^2 = 0.86–0.93). We downloaded 10 min interval $PM_{2.5}$ data between 2019 and 2020 from the PurpleAir network using the ThingSpeak's API provided by the PurpleAir company.[18] Hourly average $PM_{2.5}$ was computed by averaging the 10 min interval data. Although PurpleAir reports mass concentrations in PM_1, $PM_{2.5}$, and PM_{10}, high correlations of PM concentration between different size ranges (correlation coefficient > 0.9) were detected. $PM_{2.5}$ was selected as the target size range for this analysis, as $PM_{2.5}$ is widely used as the PM standard by U.S. Environmental Protection Agency and has been associated with most of the diseases caused or exacerbated by air pollution indoors and outdoors.[19,20]

2.3. Post-Process of PurpleAir $PM_{2.5}$ Data.

Given the importance of sensor data calibration and quality control, we used a two-step approach to post-process hourly PurpleAir $PM_{2.5}$ data to minimize the impact of sensor malfunction, intrasensor bias, and environmental and operational parameter impact. This approach applied (1) systematic quality control and (2) calibration with reference monitors.

2.3.1. Systematic Quality Control.—A comprehensive description of the quality control method used in this study can be found in Lu et al.[16] More details including various statistical indicators can be found in the Supporting Information. In summary, the systematic quality control consists of five steps below:

1. Remove malfunctioning sensor data based on a low frequency of change (i.e., 5 h moving standard deviation of zero) in their readings across time.
2. Discard apparent $PM_{2.5}$ outliers with extreme hourly values greater than 500 $\mu g \cdot m^3$ exceeding the sensor's effective measurement range in both channels or readings higher than 3 times[21] of calculated median absolute deviation by one channel within a calendar month.

3. Identify periods of prolonged interruption or data loss due to power outages or data communication loss using a 75% completeness criterion (four or more 10 min measures per hour and 18 h or more in a day).

4. Evaluate the degree of agreement from dual-channel readings for each sensor within a given month of operation based on calculated statistical anomaly detection indicators as the coefficient of determination $R^2 > 0.8$ and mean absolute error < 4. Given the reported low performance (saturate) of PurpleAir sensors at high particle concentrations (>50 $\mu g \cdot m^{-3}$), leading to higher measurement bias and uncertainty in the mean absolute error indicator, mean absolute percentage error > 0.3 was adopted as an additional criterion to handle the sensor's measurement limit at high particle concentrations.

5. In case of sensor data reported only from one channel, a linear regression of hourly readings for each sensor with its neighboring sensors within 3 km was performed and data from sensors with $R^2 < 0.6$ or having no neighboring sensors within 3 km was discarded from the analysis.

Following these steps, 1.9, 0.6, 11.2, 2.6, and 0.8% (17.2% in total) of the initial 2 796 035 hourly averaged $PM_{2.5}$ data from 139 paired indoor and outdoor sensors across California were discarded after the first, second, third, fourth, and fifth steps, respectively. Table S1 also shows the percentage of discarded data based on each period and region. Overall, the regression of U.S. EPA's air quality system (AQS) data against the original sensor data had an R^2 of 0.65 and a slope of 0.75; more spikes were also detected in the original sensor data against AQS data with a high bias of 1.2 $\mu g \cdot m^{-3}$. The quality-controlled data ($N = 2\,320\,709$) had a more robust dual-channel agreement with the AQS data (R^2: 0.95; slope: 0.98). These results agree with Bi et al.'s work that showed stronger statistical agreement with AQS data based on the quality-controlled sensor data.

2.3.2. Indoor and Outdoor Sensor Calibration.—After the systematic quality control of the data for both indoor and outdoor sensors, we used a spatially varying calibration method developed by Bi et al. for outdoor sensor data calibration. Greater details on this calibration method can be found elsewhere.[15] In short, using the data from paired outdoor PurpleAir low-cost sensors with AQS regulatory stations (54 of outdoor sensors with 26 co-located AQS within 500 m[15] radius distance in California during January–July in both 2019 and 2020), geographically weighted regression (GWR) was used to calibrate the sensor $PM_{2.5}$ data after the systematic quality control using temperature and relative humidity (RH) data from individual sensor recording as covariates.[15] In addition, to account for the quality degradation over time,[9,10,12,14,16] the total operating time of a sensor (the duration between the measurement time and the installation time) was used to adjust the effect of sensor aging.[15] Finally, the sensor uptime (the time during which a sensor is in consecutive operation from the last boot time) was used to adjust the potential impact of sensor's operational stability on data quality. A linear GWR regression was used to describe the relationship between the bias of PurpleAir measurements and four covariates[15]

$$\begin{aligned}\mathrm{AQSPM}_{2.5i} &= \beta_0(u_i, v_i) + \beta_1(u_i, v_i)\,.\ \mathrm{PurpleAir\ PM}_{2.5i} \\ &+ \beta 2(u_i, v_i) \cdot T_i + \beta_3(u_i, v_i) \cdot \mathrm{RH}_i \\ &+ \beta_3(u_i, v_i)\,.\ \mathrm{optime}_{\ i} + \beta_4(u_i, v_i)\,.\ \mathrm{uptime}_{\ i} \\ &+ \epsilon_i\end{aligned} \tag{1}$$

where $\beta(u_i, v_i)$ indicates the vector of the location-specific parameter estimates and (u_i, v_i) represents the geographic coordinates of location i. AQS $PM_{2.5i}$ and PurpleAir $PM_{2.5i}$ are the paired hourly $PM_{2.5}$ measurements at location i. T_i, RH_i, $optime_i$, and $uptime_i$ represent temperature, relative humidity, operating time, and uptime of the PurpleAir sensor at location i, respectively. The GWR was fitted using the R package "GWmodel" version 2.0. Finally, we compared the mean absolute differences of hourly measurements between 54 outdoor sensors and 26 AQS stations in both 2019 and 2020 based on $PM_{2.5}$ measurement ranges after and before calibration.

While we were able to correct outdoor sensor data using the approach above, there was no single reference monitoring instrument (federal reference method (FRM) or federal equivalent method (FEM)) indoors to repeat such a process for indoor sensor calibration. A study in Korea by Kim et al. developed average correction factors for indoor PurpleAir sensor measurements using a side-by-side sensor and reference devices (two devices; 2 weeks of sampling) and stepwise linear regression. While to some extent major indoor sources may differ in our study vs those in Korea, we used the average correction factor for indoor sensor data reported by Kim et al. because of the lack of such data in California. Further, four (two in northern California and two in southern California) of the paired outdoor-AQS monitors were collocated with indoor sensors,[22] allowing us to, at least, determine the change in the indoor–outdoor correlation coefficient and slope on a rather small scale (i.e., four indoor–outdoor pairs of sensors) after applying the indoor sensor correction factor from Kim et al.

2.4. Data Analysis.

Daily average $PM_{2.5}$ was computed by averaging hourly calibrated data based on the two-step post-process described in Section 2.3. The daily data were grouped into pre-, during, and post-lockdown periods for all subsequent analyses. Daily temporal variation of $PM_{2.5}$ concentrations in 2020 was plotted and overlaid with concentrations in 2019 in two subregions. The average diurnal variation of indoor concentrations was investigated to help identify potential emission sources and the time periods with a high probability of indoor sources. Inside/outside $PM_{2.5}$ concentration (I/O) ratios were calculated on a daily basis to examine the hypothesis of increased I/O ratios during the lockdown period.

The sources of the indoor particulate matter can be decomposed into two parts,[21] one produced by indoor sources and the other from the infiltration of outdoor air into the indoor environment. To better understand the relationship between indoor and outdoor $PM_{2.5}$ and potential indoor sources, we described indoor $PM_{2.5}$ concentration as follows[22]

$$C_{\mathrm{i}} = C_{\mathrm{og}} + C_{\mathrm{ig}} = C_{\mathrm{o}} \cdot F_{\mathrm{INF}} + C_{\mathrm{ig}} \tag{2}$$

where C_i is the daily average indoor $PM_{2.5}$ concentration, C_{ig} is the sum of indoor-generated $PM_{2.5}$ ($\mu g \cdot m^{-3}$), C_{og} represents the outdoor-generated $PM_{2.5}$ that has penetrated indoors and remains suspended ($\mu g \cdot m^{-3}$), and C_{og} is the product of the daily average outdoor concentration (C_o, $\mu g \cdot m^{-3}$) and the infiltration factor (F_{INF}, dimensionless). F_{INF} is a dimensionless factor that is a function of housing and atmospheric characteristics. Since we did not take any systematic measurements of F_{INF} during this study, we followed an established regression model method[23] to derive the F_{INF} and C_{ig} in pre-, during, and post-shutdown periods. In brief, the indoor and outdoor particle infiltration coefficient was obtained by the linear regression model also known as the random component superposition model (RCS) between C_i and C_o. The contribution of indoor-generated $PM_{2.5}$ to overall indoor $PM_{2.5}$ concentrations (C_{ig}/C_i) was also calculated. Standard errors (SE) associated with daily C_i and C_o were used to derive the uncertainty associated with the derived C_{ig}.

Multisensor deployment inside a house could shed light on the spatiotemporal variation of pollutant concentrations and source emissions, as well as ventilation efficiency and pollutant dispersion and decay in different compartments of the house.[24–27] To better understand $PM_{2.5}$ variation and potential emission sources in different locations of a house, we examined the multiple indoor sensor data in a residential house located in a remote-background area in Aromas, Monterey County (Figure S1). We calculated the fraction of indoor source-generated $PM_{2.5}$ to the total indoor $PM_{2.5}$ in different indoor locations and summarized the results by diurnal time periods, which may indicate certain activities that contribute to indoor sources (e.g., cooking).

3. RESULTS AND DISCUSSION

3.1. Spatially Varying Sensor Correction Factors for Outdoor PurpleAir $PM_{2.5}$.

A linear regression of uncalibrated but quality-controlled PurpleAir measurements against AQS had an R^2 of 0.82 and a slope of 0.74. Compared to measurements from 26 AQS monitors in this study, the PurpleAir data showed site-specific R^2 ranging from 0.23 to 0.90 and the site-specific slope from 0.34 to 0.94. The observed variations between the PurpleAir and AQS data were less pronounced than those reported by Bi et al.

The GWR slopes of PurpleAir (β_1 in eq 1) averaged 0.53 with an interquartile range of 0.03. The largest slope was 0.57. After calibration, the overall systematic bias of PurpleAir decreased from 1.2 to 0.1 $\mu g \cdot m^{-3}$. The overall PurpleAir residual error was also reduced, reflected in a decreased standard deviation of the AQS and PurpleAir differences from 6.02 to 4.10 $\mu g \cdot m^{-3}$ (i.e., a 32% decrease). The calibration model had a 10-fold CV R^2 of 0.89 for the AQS and PurpleAir data, which is higher than the R^2 of 0.83 for uncalibrated data, indicating the improvement of the overall precision of PurpleAir data. Since the environmental conditions were similar between our study and Bi et al.'s work, we relied on the results reported by Bi et al. for the generalized additive model-fitted relationships of the AQS and PurpleAir absolute differences and temperature, RH, operating time, and uptime.

In terms of indoor sensor calibration, after applying the correction factor developed by Kim et al., indoor–outdoor correlation coefficients and slopes and subsequent results on

indoor-generated $PM_{2.5}$ did not change significantly, suggesting a minimal effect of indoor relative humidity and temperature on sensor readings.

3.2. Spatial and Temporal Variation of Calibrated Indoor and Outdoor $PM_{2.5}$ Across California.

Figure 2 compares daily $PM_{2.5}$ concentrations indoors and outdoors as well as I/O ratios for pre-, during, and post-lockdown periods. Overall, concentrations during the pre-lockdown period in 2020 were not significantly different from those in the same months in 2019 (0–10% difference by the subregion and for both indoor and outdoor levels, *p*-value = 0.1–0.2). This suggests that the main emission sources and atmospheric conditions were similar in 2020 and 2019 before social distancing measures were in place. Outdoor $PM_{2.5}$ concentrations are lower during the COVID-19 lockdown period compared to those of the pre-lockdown period in 2020. While outdoor $PM_{2.5}$ levels were lower in northern California in comparison to southern California during the lockdown (4.1 $\mu g \cdot m^{-3}$ vs 5.8 $\mu g \cdot m^{-3}$), indoor levels were higher in northern California than southern California (5.1 $\mu g \cdot m^{-3}$ vs 3.5 $\mu g \cdot m^{-3}$) during the same period. These might suggest that stricter measures for work-from-home policies and stay-at-home orders in northern California[28,29] may have increased indoor activities and related emissions. County-level google mobility data also confirms a sharper increase in residential mobility in Northern California Counties, especially San Francisco and Sacramento counties in comparison to Southern counties in California (Figures S1 and S2). The sharper increase in I/O ratios from pre-lockdown to lockdown period in Northern California (from 0.8 to 1.4) in comparison to Southern California (from 0.5 to 0.7) also supports this hypothesis. On the other side, outdoor $PM_{2.5}$ levels dropped drastically (by 20–40%) following the urban activity restriction, with a sharper decrease detected in Southern California than Northern California. This was expected given the more concentrated contribution of traffic-related PM in metropolitan areas in the southern part of the state, especially in Los Angeles county.[13,14] Finally, post-lockdown I/O ratios increased 23–35% in comparison to the same period in 2019 across California, suggesting consistently elevated indoor air pollution when some people continued to work/study remotely.

3.3. Diurnal Variation of Indoor $PM_{2.5}$.

Figure 3 shows average indoor and outdoor hourly $PM_{2.5}$ concentrations by different types of sites during and post-lockdown periods in 2020 and 2019. It should be noted that diurnal variation of indoor $PM_{2.5}$ in the pre-lockdown period (January 1–March 16) was similar (*p*-value = 0.1) in 2020 and 2019 (Figure S4). Diurnal variation of indoor $PM_{2.5}$ concentrations in remote residential sites showed a clear peak during the noon–3 pm period and remained high in the afternoon/evening. This reflects enhanced human activity during lunchtime (i.e., cooking) and work-from-home activities that increase particle resuspension in homes. Household cleaning products are a particularly relevant source of indoor pollution at this juncture in the time given that many people may be cleaning more frequently and use stronger disinfectants to reduce viral infection.[30] Also, the afternoon peak in 2020 was more pronounced, reaching a maximum of 10 $\mu g \cdot m^{-3}$ in comparison to the maximum of 6 $\mu g \cdot m^{-3}$ in 2019. Moreover, the afternoon peak occurred slightly later in the residential sites close to major roads than in the remote residential sites away from traffic (1–5 pm vs 12–3 pm), which partially reflects the delayed impact of early afternoon traffic on the

sites close to traffic (Figure 3). All residential sites experienced an elevated afternoon peak toping at roughly 10 $\mu g \cdot m^{-3}$. An increasing trend was also observed in indoor $PM_{2.5}$ concentrations after traffic rush hours (i.e., 8 pm–midnight) on the residential sites close to traffic. While unknown indoor source emissions could play a role on late-night elevated indoor $PM_{2.5}$, higher infiltration ratios due to more open window circulation after traffic hours near roadways might be another potential reason for such an increasing trend. In the case of office/school sites, no significant diurnal fluctuations were observed in 2020, mainly due to the lockdown and closed or inactive business. Unlike residential sites, the office/school site showed markedly higher $PM_{2.5}$ concentrations during the baseline scenario in 2019 with a clear peak around early afternoon time.

3.4. Indoor-Generated $PM_{2.5}$ in Pre-, During, and Post-Lockdown Periods.

Table 2 describes the relations of indoor and outdoor $PM_{2.5}$ concentrations and the contribution of indoor emission sources to indoor $PM_{2.5}$ by the types of sites. The Pearson correlation coefficient between indoor and outdoor concentrations ranged from 0.4 to 0.7, with higher correlations in the pre-lockdown period in comparison to during and post-lockdown periods in residential units. The correlation coefficients for office/school sites almost remained at a moderate level and changed slightly before, during, and after the lockdown, probably because a reduction in both outdoor and indoor $PM_{2.5}$ sources occurred during and after the lockdown. On average, the infiltration rates (F_{INF}) were lowest in background residences (0.5), followed by near-road residences (0.6), and the highest in near-road office/school buildings (0.7). This is probably because offices and classrooms have more powerful ventilation systems deployed, and background residences identified in our study may be newer and more air-tight than those near-roadway ones, which agree with previous studies in a similar setup.[22,23] Future work is needed to confirm these hypotheses with detailed building characteristics information. Slightly lower infiltration rates (less than 10%) were observed during the lockdown periods compared to the other periods in 2020. This is possibly because people went outside less frequently (thus less door-opening activities) during the lockdown.

The percent contribution of indoor-generated $PM_{2.5}$ to indoor concentration (C_{ig}/C_i) was in the range of 23–35% in the pre-lockdown periods, with higher rates observed in residential-background sites. This baseline scenario is consistent with a similar observation of a previous study that shows 21–33% on average.[23] However, the contribution of indoor sources drastically increased during and after lockdown in the residential sites, especially those located in the remote-background area (p-value = 0.04). For example, in residential-background sites, on average, C_{ig}/C_i increased from 34.2% in the pre-lockdown period to as high as 80% during the lockdown (almost a 3-fold increase) (p-value = 0.03) and then slightly decreased in the reopening stage to 67.4%. The absolute contribution of indoor sources suggests a consistent and statistically significant increase in indoor-generated $PM_{2.5}$ during the stay-at-home orders in the residential setting, with the highest average increase of 3.9 $\mu g \cdot m^{-3}$ during the lockdown for background residences. C_{ig}/C_i dropped slightly in office/school sites during- and after lockdown compared to the pre-lockdown period, reflecting reduced indoor activities during these periods although the magnitude of reduced indoor emissions is smaller than expected. Little change was observed for the absolute

value of indoor-generated $PM_{2.5}$ in near-road office/school sites (p-value = 0.21), probably because this contribution was small to start with (1.3 $\mu g \cdot m^{-3}$) in the pre-lockdown period and because of the uncertainty in deriving the contribution of indoor sources.

3.5. Case Study of a House with Multiple Indoor Sensors.

We explored indoor $PM_{2.5}$ trends in different compartments of a residential unit located in a remote-background area (Figure S1). Two of the four indoor sensors were deployed in the dinning and kitchen area and the remaining two were in the living and bedrooms. We have grouped the sensors into "dining/kitchen" and "living/bedrooms" as no significant difference was detected within each group of sensors. The co-located outdoor sensor was located in the front porch of the house and was labeled as "Front porch (outdoor)". Peaks in C_{ig}/C_i in the dining/kitchen area were strongly associated with expected breakfast/lunch/dinner periods (i.e., 7–9 am, 12–2 pm, 5–8 pm) during the day (Figure 4). Further, living/bedrooms sensors showed relatively higher contribution from indoor sources during evening time (i.e., 5–8 pm), likely due to after work/school cleaning activities that generate new particles, more people and movement that suspend particles, and more dispersion of PM from dining/kitchen from people's movement and behavior (e.g., open bedroom doors) that increases air exchange within the house. Daily temporal variation of $PM_{2.5}$ levels from January 1 to July 30, 2020 recorded by sensor sets can be found in Figure S5a,b. While outdoor levels were 30–44% higher than those in dining/kitchen areas in the pre-lockdown period, dining/kitchen levels were almost comparable with or higher than the outdoor levels during the lockdown, suggesting an extraordinary increase in cooking and dining activities during the lockdown. In all of the time periods (pre-, during, and post-lockdown), concentrations in living/bedrooms were lower than those in dining/kitchen.

The existing indoor–outdoor PurpleAir sensor network enabled us to detect and characterize increases in indoor-generated $PM_{2.5}$ in residences due to the stay-at-home orders and telecommuting. We found higher absolute indoor $PM_{2.5}$ concentrations and as high as 80% increase in the contribution of indoor-generated $PM_{2.5}$ to total indoor concentrations during and post-lockdown periods. While the current study lacks detailed time activity information and co-pollutant measurements, it highlights elevated indoor emission sources and worsened indoor air quality during the COVID era due to increased indoor activities. This study points to potential public health implications as more people are expected to work/study from home in the future compared to the pre-COVID time.

3.6. Study Strength and Limitations.

Our current study is the first to investigate indoor–outdoor air quality in a large spatial scale using low-cost sensor networks with a diurnal variation of $PM_{2.5}$ concentrations. The strengths of this study include large sample size across the entire State of California, use of spatial and temporal comprehensive sensor data with thorough calibration and correction, and investigation of both indoor and outdoor $PM_{2.5}$ variations levels pre-, during, and post-COVID lockdown. Several limitations also exist. While our result can shed light on the indoor-generated $PM_{2.5}$ pre-, during, and post-COVID-19 lockdown, there are uncertainties associated with the indoor sensor calibration given the lack of the co-located indoor sensor and reference device in any of the PurpleAir site across California. Our study also did not

provide any systematic analysis on the building types, ventilation systems, and their effect of infiltration ratios to calculate indoor-generated $PM_{2.5}$ with lower associated uncertainties. Based on the data analysis, we suspect that the ventilation system in offices/schools may have been on during the lockdown period. Further, the increased infiltration rate during the post-lockdown period could likely be attributed to more human activities (e.g., open door and window) and warmer season that increases natural ventilation. Nevertheless, our study has strong public health implications as it highlights the increase in residential indoor air pollution levels due to more indoor emissions as more people are expected to work/study from home in the future compared to the pre-COVID time.

Supplementary Material

Refer to Web version on PubMed Central for supplementary material.

ACKNOWLEDGMENTS

This study was supported by the National Institute of Environmental Health Sciences (NIEHS #ES030353). The authors are also grateful for the PurpleAir company in making the sampling data publicly available. The authors also appreciate numerous PurpleAir sensor users who did the monitoring and connectively contributed to the measurement data and made this research feasible.

REFERENCES

(1). Chandrasekaran B; Fernandes S Since January 2020 Elsevier Has Created a COVID-19 Resource Centre with Free Information in English and Mandarin on the Novel Coronavirus. The COVID-19 Resource Centre Is Hosted on Elsevier Connect, the Company' s Public News and Information Website. Diabetes Metab. Syndr 2020, 14, 337–339. [PubMed: 32305024]

(2). Forster PM; Forster HI; Evans MJ; Gidden MJ; Jones CD; Keller CA; Lamboll RD; Quéré C; Le; Rogelj J; Rosen D; Schleussner C; Richardson TB; Smith CJ; Turnock ST Current and future global climate impacts resulting from COVID-19. Nat. Clim. Change 2020, 10, 913–919.

(3). Tanzer-Gruener R; Li J; Eilenberg SR; Robinson AL; Presto AA Impacts of Modifiable Factors on Ambient Air Pollution: A Case Study of COVID-19 Shutdowns. Environ. Sci. Technol. Lett 2020, 7, 554–559.

(4). He G; Pan Y; Tanaka T The short-term impacts of COVID-19 lockdown on Urban Air Pollution in China. Nat. Sustainability 2020, 3, 1005–1011.

(5). Berman JD; Ebisu K Science of the Total Environment Changes in U. S. Air Pollution during the COVID-19 Pandemic. Sci. Total Environ 2020, 739, No. 139864. [PubMed: 32512381]

(6). Giani P; Castruccio S; Anav A; Howard D; Hu W; Crippa P Short-Term and Long-Term Health Impacts of Air Pollution Reductions from COVID-19 Lockdowns in China and Europe: A Modelling Study. Lancet Planet. Health 2020, 4, e474–e482. [PubMed: 32976757]

(7). WHO. Household Air Pollution and Health, May 8, 2018. https://www.who.int/news-room/fact-sheets/detail/household-air-pollution-and-health.

(8). Kumar P; Morawska L; Martani C; Biskos G; Neophytou M; Di Sabatino S; Bell M; Norford L; Britter R The Rise of Low-Cost Sensing for Managing Air Pollution in Cities. Environ. Int 2015, 75, 199–205. [PubMed: 25483836]

(9). Ardon-Dryer K; Dryer Y; Williams JN; Moghimi N Measurements of PM2.5 with PurpleAir under Atmospheric Conditions. Atmos. Meas. Tech 2020, 13, 5441–5458.

(10). Sayahi T; Butterfield A; Kelly KE Long-Term Field Evaluation of the Plantower PMS Low-Cost Particulate Matter Sensors. Environ. Pollut 2019, 245, 932–940. [PubMed: 30682749]

(11). Gupta P; Doraiswamy P; Levy R; Pikelnaya O; Maibach J; Feenstra B; Polidori A; Kiros F; Mills KC Impact of California Fires on Local and Regional Air Quality: The Role of a Low-Cost Sensor Network and Satellite Observations. GeoHealth 2018, 2, 172–181. [PubMed: 31157310]

(12). Feenstra B; Papapostolou V; Hasheminassab S; Zhang H; Der Boghossian B; Cocker D; Polidori A Performance Evaluation of Twelve Low-Cost PM2.5 Sensors at an Ambient Air Monitoring Site. Atmos. Environ 2019, 216, No. 116946.

(13). Barkjohn KK; Gantt B; Clements AL Development and Application of a United States Wide Correction for PM2.5 Data Collected with the PurpleAir Sensor. Atmos. Meas. Tech 2020, 2020, 1–34.

(14). Stavroulas I; Grivas G; Michalopoulos P; Liakakou E; Bougiatioti A; Kalkavouras P; Fameli KM; Hatzianastassiou N; Mihalopoulos N; Gerasopoulos E Field Evaluation of Low-Cost PM Sensors (Purple Air PA-II) Under Variable Urban Air Quality Conditions, in Greece. Atmosphere 2020, 11, No. 926.

(15). Bi J; Wildani A; Chang HH; Liu Y Incorporating Low-Cost Sensor Measurements into High-Resolution PM2.5 Modeling at a Large Spatial Scale. Environ. Sci. Technol 2020, 54, 2152–2162. [PubMed: 31927908]

(16). Lu Y; Giuliano G; Habre R Estimating Hourly PM2.5 Concentrations at the Neighborhood Scale Using a Low-Cost Air Sensor Network: A Los Angeles Case Study. Environ. Res 2021, 195, No. 110653. [PubMed: 33476665]

(17). California Department of Public Health. Regional Stay At Home Order, 2020.

(18). South Coast Air Quality Management District (SCAQMD). Field Evaluation PurpleAir (PA-II) PM Sensor, 2017. http://www.aqmd.gov/Docs/Default-Source/Aq-Spec/Field-Evaluations/Purple-Air-Pa-Ii---Field-Evaluation.Pdf?Sfvrsn=4.

(19). Beelen R; Hoek G; van den Brandt PA; Goldbohm RA; Fischer P; Schouten LJ; Jerrett M; Hughes E; Armstrong B; Brunekreef B Long-Term Effects of Traffic-Related Air Pollution on Mortality in a Dutch Cohort (NLCS-AIR Study). Environ. Health Perspect 2008, 116, 196–202. [PubMed: 18288318]

(20). Pope CA III; Burnett RT; Thun MJ; Calle EE; Krewski D; Thurston GD To Fine Particulate Air Pollution. J. Am. Med. Assoc 2002, 287, 1132–1141.

(21). Miller J Reaction Time Analysis with Outlier Exclusion: Bias Varies with Sample Size. Q. J. Exp. Psychol 1991, 43, 907–912.

(22). Kim S; Park S; Lee J Evaluation of Performance of Inexpensive Laser Based PM2.5 Sensor Monitors for Typical Indoor and Outdoor Hotspots of South Korea. Appl. Sci 2019, 9, No. 1947.

(23). Lv Y; Wang H; Wei S; Zhang L; Zhao Q The Correlation between Indoor and Outdoor Particulate Matter of Different Building Types in Daqing, China. Procedia Eng 2017, 205, 360–367.

(24). Meng QY; Turpin BJ; Jong HL; Polidori A; Weisel CP; Morandi M; Colome S; Zhang J; Stock T; Winer A How Does Infiltration Behavior Modify the Composition of Ambient PM 2.5 in Indoor Spaces? An Analysis of RIOPA Data. Environ. Sci. Technol 2007, 41, 7315–7321. [PubMed: 18044505]

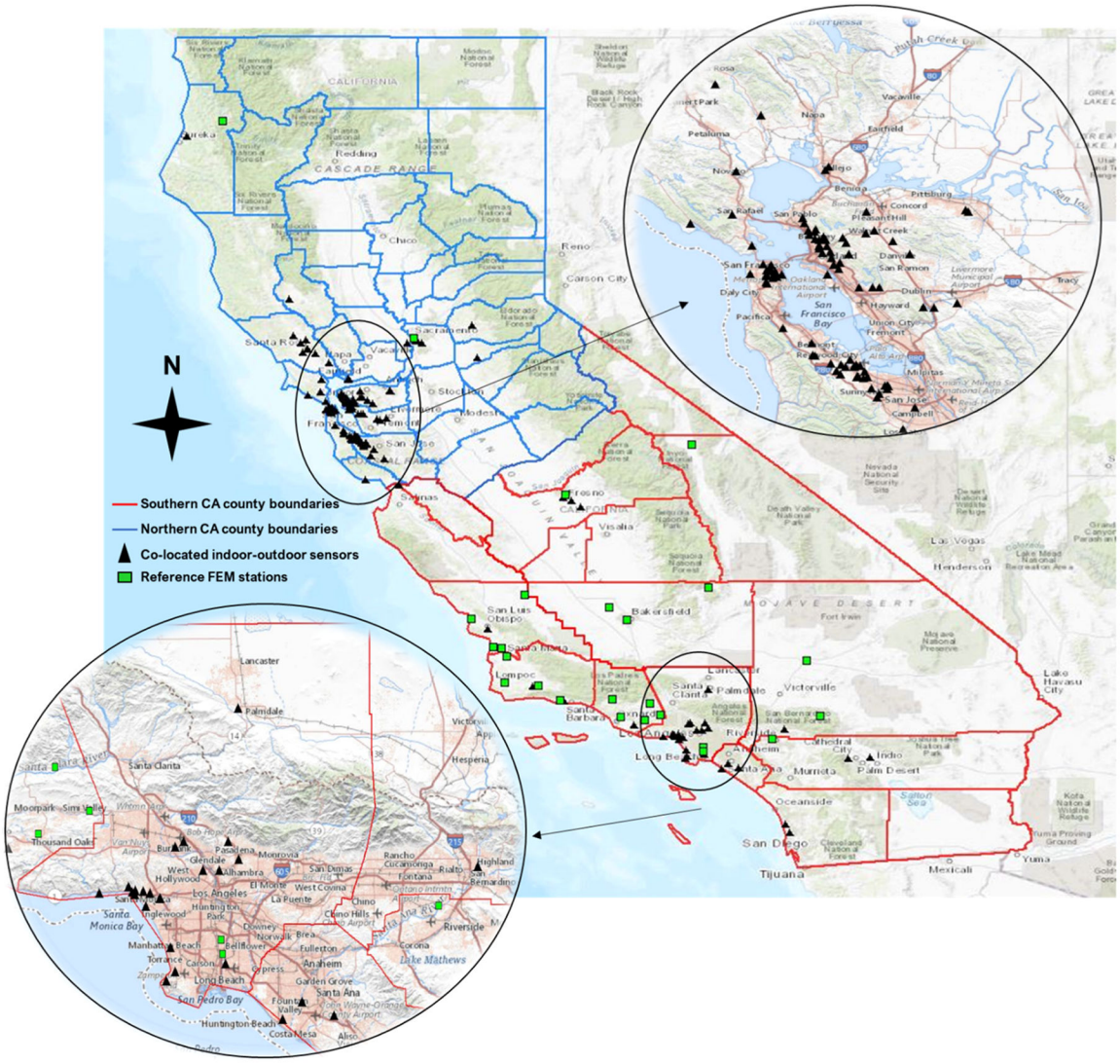

Figure 1.

Map of sites with operational co-located PurpleAir sensors and reference FEM stations in California during January 2019–July 2020.

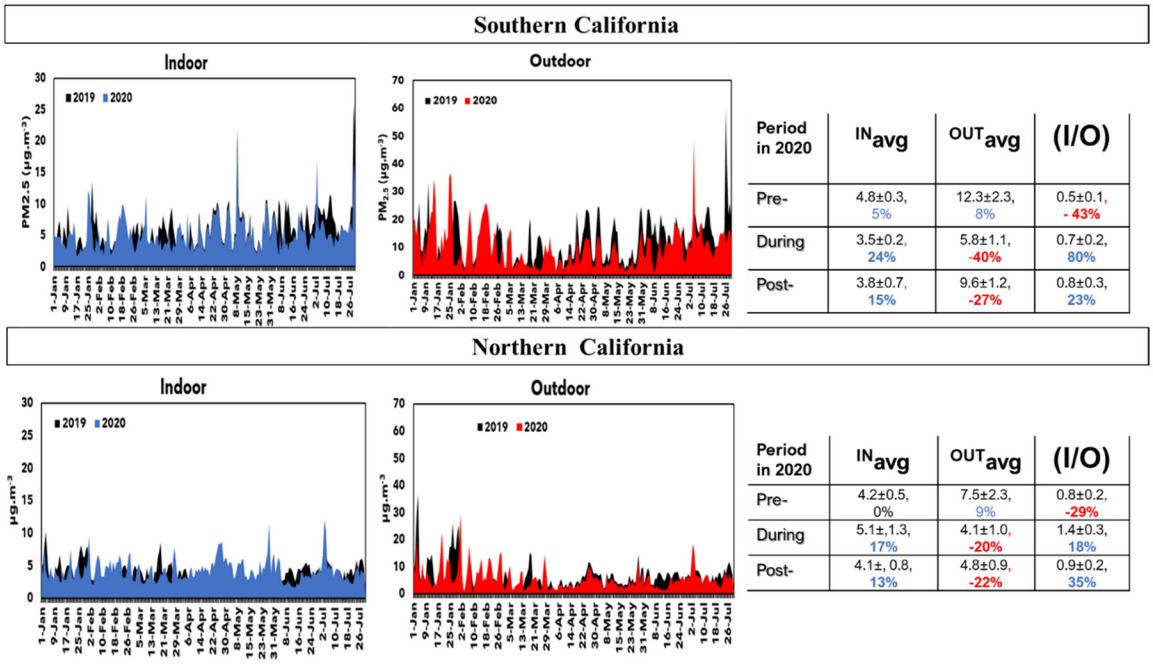

Figure 2.

Temporal variation of indoor and outdoor $PM_{2.5}$ (daily average) in southern and northern California in pre-, during-, and post- lockdown periods in 2020 and the same time periods in 2019. Average indoor (IN_{avg}) and outdoor (OUT_{avg}) $PM_{2.5}$ concentrations ($\mu g \cdot m^{-3}$) and indoor-to-outdoor ratios (I/O) for each time period are in the right panel tables. Percentages in the tables show the percent of change (increase in blue and decrease in red) in comparison to 2019 levels during the same period. All of the percent increase/decrease in bold in the table were statistically significant (p-value < 0.05). Values associated with ± are standard error (SE) of the daily sensor readings.

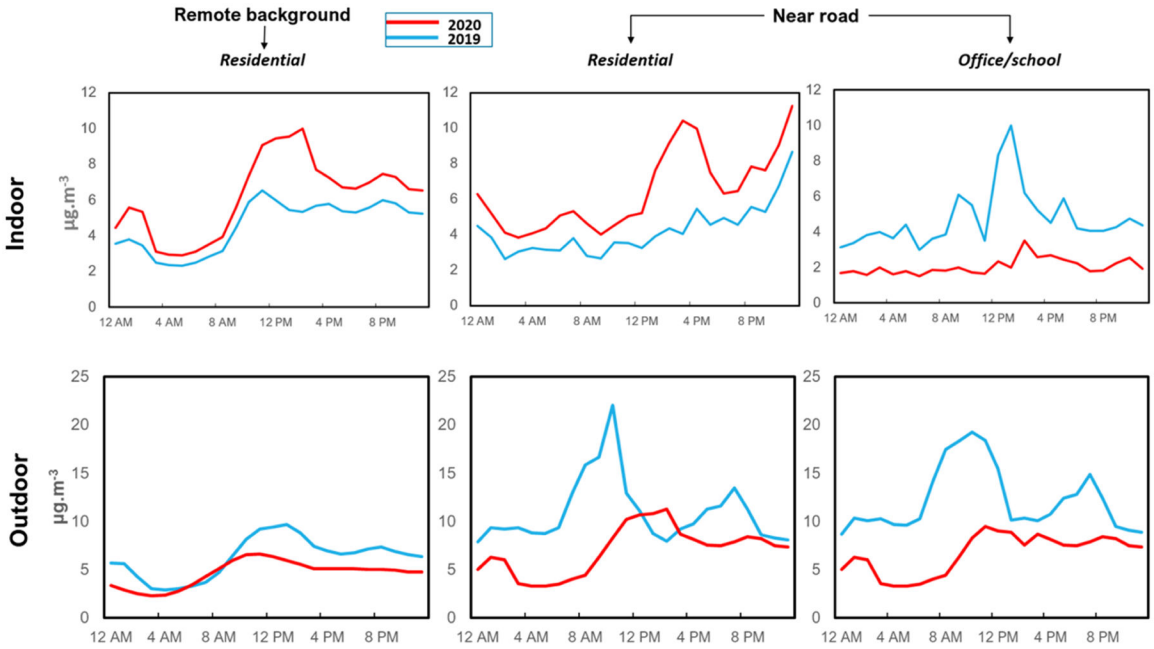

Figure 3.

Diurnal variation of indoor and outdoor $PM_{2.5}$ (10 min average across multiple sites) in selected co-located sensor sets of different types of sites across California from March 16 to July 30 (lockdown and post-lockdown periods) in both 2020 and 2019 (business as usual).

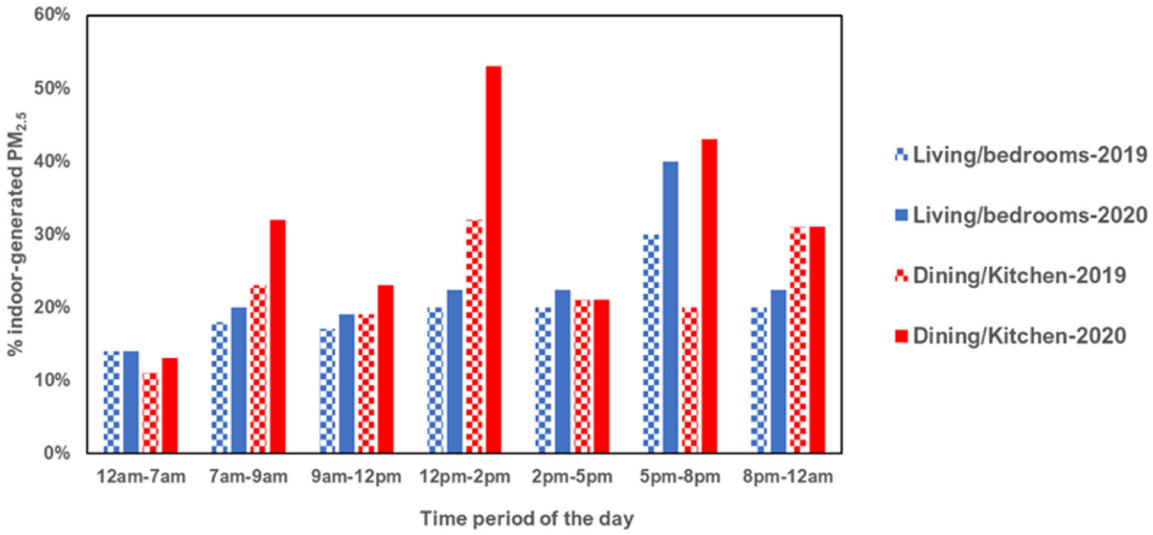

Figure 4.

Percent contribution of indoor-generated $PM_{2.5}$ to average total indoor concentration in a residential house with multiple indoor sensors during different time periods of the day.

Table 1.

Summary of Co-Located Indoorand Outdoor Sites

type of sites	southern California	northern California
residential—remote background[a]	34 (*N* = 577 655)	32 (*N* = 506 543)
residential—near road[b]	24 (*N* = 394 100)	16 (*N* = 267 300)
office/school—near road	22 (*N* = 377 400)	11 (*N* = 193 711)
total	80 (*N* = 1 349 155)	59 (*N* = 967 543)

[a]Remote-background sites are located more than 50 m from the edge of the major emissions sources.

[b]Sites near a major freeway or main street are labeled as the near-road site impacted by traffic emissions.

Table 2.

Pearson Correlation Coefficients Between the Indoor and Outdoor $PM_{2.5}$, Filtration Ratio (F_{INF}) Derived from the Regression Model, Sum of Indoor-Generated $PM_{2.5}$ (C_{ig}), and Percent Contribution of Indoor-Generated $PM_{2.5}$ to Total Indoor $PM_{2.5}$ Mass Concentrations (C_{ig}/C_i) for Co-Located Sites by Different Site Types in Pre-, During, and Post-Lockdown Periods in 2020

	Pearson correlation coefficient for indoor–outdoor concentrations			**F_{INF}**			**C_{ig} ($\mu g \cdot m^{-3}$)**			**C_{ig}/C_i (%)**		
site type	**pre**	**during**	**post**	**pre**	**during**	**post**	**pre**	**during**	**post**	**pre**	**during**	**post**
residential—near road	0.8	0.5	0.6	0.6	0.6	0.7	1.2	2.3	2.5	**23.4**	**52.4**	**43.2**
residential-background	0.7	0.6	0.5	0.6	0.5	0.6	1.6	2.7	2.9	**29.1**	**75.1**	**69.4**
office/school—near road	0.6	0.6	0.6	0.5	0.8	0.6	1.3	1.0	1.1	**25.6**	**21.7**	**23.3**